DESIGN OF IOT-BASED GREENHOUSE MONITORING AND CONTROL SYSTEM USING ADAPTIVE PARTICLE SWARM OPTIMIZED FUZZY PID CONTROLLER AND VISUALIZATION PLATFORM

/

基于自适应粒子群优化模糊 PID 控制器和可视化平台的物联网温室监控系统设计

Peiyu LIN [1,2,3)], Rui XU [1,2,3)], Haifang WANG [4)], Jingcheng HUANG [1,2,3)], Zhen GUO [1,2,3)], Xia SUN [1,2,3)], Ibrahim A. DARWISH [5)], Yemin GUO [*1,2,3)], Jicheng ZHAO [*1,2,3)]

[1)] College of Agricultural Engineering and Food Science, Shandong University of Technology, No. 266 Xincun Xilu, Zibo, Shandong 255049, China;

[2)] Shandong Provincial Engineering Research Centre of Vegetable Safety and Quality Traceability, No. 266 Xincun Xilu, Zibo, Shandong 255049, China;

[3)] Zibo City Key Laboratory of Agricultural Product Safety Traceability, No. 266 Xincun Xilu, Zibo, Shandong 255049, China

[4)] Wangjing Hospital, China Academy of Chinese Medical Sciences, Beijing 100102, China;

[5)] Department of Pharmaceutical Chemistry, College of Pharmacy, King Saud University, P.O. Box 2457, Riyadh 11451, Saudi Arabia

**Corresponding authors: Professor Yemin GUO and Jicheng ZHAO*

Tel: +86-533-2786398; E-mail: gym@sdut.edu.cn; zhaojicheng@sdut.edu.cn

DOI: https://doi.org/10.35633/inmateh-75-100

Keywords: *internet of things, fuzzy PID control, adaptive particle swarm optimization algorithm, smart agriculture, greenhouse control*

ABSTRACT

Traditional greenhouse management often suffers from slow responsiveness and limited adaptability due to its reliance on manual operations. This study proposes a greenhouse environment monitoring and control system that integrates Internet of Things (IoT) technologies with a fuzzy PID controller optimized through an Adaptive Particle Swarm Optimization (APSO) algorithm. A real-time monitoring platform was developed based on a WebSocket-enabled front-end/back-end separation architecture. Environmental parameters, such as temperature and humidity, were collected by sensors and transmitted in real time to the platform via the MQTT protocol, enabling data visualization and anomaly detection. The APSO algorithm was employed offline to optimize the fuzzy PID parameters, and the resulting controller was implemented on a microcontroller to achieve real-time control. Compared with conventional PID control, the APSO-optimized controller reduced overshoot by 72.1% and shortened the settling time by 20%. Experimental results demonstrated that the system was less susceptible to external environmental disturbances, maintaining temperature fluctuations within 0.3°C. This study provides a robust and effective solution for smart greenhouse management.

摘要

由于依赖人工操作，传统的温室管理往往存在响应速度慢、适应性有限等问题。本研究提出了一种温室环境监测和控制系统，该系统将物联网（Internet of Things, IoT）技术与通过自适应粒子群优化（Adaptive Particle Swarm Optimization, APSO）算法优化的模糊 PID 控制器相结合。提出基于 WebSocket 的前端/后端分离架构，开发了一个实时监控平台。温度和湿度环境参数由传感器收集，并通过 MQTT 协议实时传输到平台，从而实现数据可视化和异常检测。采用 APSO 算法离线优化模糊 PID 参数，并在微控制器上实现控制器的实时控制。与传统的 PID 控制相比，APSO 优化控制器将过冲降低了 72.1%，并将稳定时间缩短了 20%。实验结果表明，该系统不易受外部环境干扰的影响，能将温度波动保持在 0.3°C 以内。本研究为智能温室管理提供了一个稳健有效的解决方案。

INTRODUCTION

In recent years, advancements in agricultural production technologies have become increasingly critical due to the continuous growth of the global population and the rising demand for food. Predictions indicate that by 2050, the global population will reach approximately 8.52 billion, reflecting a 10.6% increase from 7.7 billion in 2020 (*Akaev, 2022*). Correspondingly, global food demand is expected to rise by nearly 60% (*van Dijk et al., 2021*). However, the agricultural sector faces escalating challenges, including limited arable land, water scarcity, and environmental concerns.

A significant portion the world's freshwater resources is used for agricultural irrigation, while a large proportion of greenhouse gas emissions can be attributed to the global food production system (*Hemathilake and Gunathilake, 2022, Khondoker et al., 2023)*. In addition, climate change has led to an increased frequency of extreme weather events, further complicating agricultural production and heightening its unpredictability (*Kumar et al., 2022*). Therefore, improving agricultural efficiency and sustainability has become imperative.

Smart agriculture, which integrates information technology, automated control, and agricultural science, has emerged as a promising solution to these challenges (*Goli et al., 2024*). Among its various applications, greenhouse cultivation plays a pivotal role in enhancing crop yield and quality by providing controlled environmental conditions (*Atia and El-madany, 2017*). Globally, over 470,000 hectares of land worldwide are dedicated to greenhouse cultivation, yielding approximately ten times more per unit area compared to open-field cultivation (*Zhou et al., 2021*). Many crops grown in greenhouses (e.g. tomatoes, strawberries, etc.) require stable temperature and humidity levels to promote optimal flowering, fruit set and ripening. Temperature deviations can adversely affect fruit quality and yield, while high humidity may increase the risk of fungal diseases. Therefore, precise microclimate control is essential for successful crop cultivation. However, traditional greenhouse control systems often struggle to maintain precise environmental regulation due to fluctuating external conditions and complex parameter interactions. Many conventional approaches lack the responsiveness and precision required for modern agricultural standards (*Katzin et al., 2022*). In particular, traditional control methods face challenges such as response delays and insufficient adjustment precision in regulating key environmental parameters like temperature and humidity concentration, making it difficult to meet the high standards of modern agriculture.

The concept of the Internet of Things (IoT) can be traced back to the 1990s (*Chin et al., 2019, Schoder, 2018*). With advancements in technology and the expansion of its applications, IoT holds the potential to revolutionize various fields, including supply chain management, logistics tracking, intelligent transportation, and environmental monitoring *(Fadhel et al., 2024*). In agriculture, IoT has emerged as a key emerging technology driving agricultural development, with widespread applications in cultivation, livestock farming, and agricultural product traceability, playing a crucial role in promoting agricultural advancement (*Gatkal et al., 2024, Mohamed et al., 2022, Omasa et al., 2022*). Wang *et al.* (*2018*) developed an IoT-based intelligent greenhouse control system that can effectively monitor the greenhouse environment. However, the cloud platform lacks analysis and algorithm control and cannot achieve accurate environmental control.

Fuzzy logic control, with its advantages in handling nonlinear and uncertain systems, has become an effective method for greenhouse environment control. Unlike traditional control methods, fuzzy logic control does not require precise mathematical models and can achieve flexible control of complex systems through fuzzy rules and fuzzy inference, making it particularly suitable for the multi-variable and highly coupled environment of greenhouses (*Cheng, 2020, Wang and Zhang, 2018, Thomopoulos et al., 2024*). *Marco A. Márquez-Vera et al.* (*2016*) developed an internal temperature control system for greenhouses based on an inverse fuzzy model. The fuzzy partitions for each climate variable used two membership functions, which enhanced the model's accuracy and response speed. The model was tuned using batch least squares and updated with recursive least squares to optimize control performance. Adaptive Particle Swarm Optimization (APSO) is an improved algorithm that introduces an adaptive mechanism to the traditional Particle Swarm Optimization (PSO) algorithm (*Zhang et al., 2014*). Different from the standard PSO algorithm, APSO dynamically adjusts the key parameters of the algorithm and automatically optimizes them based on feedback information during the search process. This improves the global search capability and helps avoid convergence to local optima. Through this adaptive mechanism, APSO can better balance global exploration and local exploitation, and enhance the convergence and search efficiency of the algorithm, which is especially suitable for complex, multi-peaked, nonlinear, and high-dimensional optimization problems (*Zheng et al., 2023*).

Based on the aforementioned background, this paper develops and tests a small greenhouse control system that integrates fuzzy PID control optimized by an APSO algorithm and an intelligent monitoring platform. The system design includes data collection from a network of sensors, parameter adjustment via a fuzzy controller, and seamless integration with the intelligent monitoring platform. The overall cost of the system is lower compared to traditional greenhouse methods, which not only improves the accuracy of environmental regulation, but also provides significant economic benefits. It can accurately control greenhouse temperature, reducing energy consumption, and the use of sensors and low-maintenance communication equipment helps to lower design costs. Furthermore, the intelligent monitoring platform minimizes manual intervention, improving management efficiency and reducing labour costs.

MATERIALS AND METHODS

Hardware equipment

In a small-scale greenhouse control system for smart agriculture, sensors are critical components for achieving real-time monitoring and control of environmental parameters (*Lee et al., 2019*). The system described in this paper utilizes a variety of devices to monitor key environmental data in the greenhouse, as shown in Table 1. The soil sensor (Model: VMS-3001-TR-*) and air sensor (Model: VMS-3002-WS) were sourced from VEMSEE flagship store (Address: Hangzhou, Zhejiang Province, China). The 8-channel RS485 hub supports multi-channel input and can connect up to 8 RS485 signal inputs, thereby enabling centralized management of data from multiple sensor devices. The system gateway was obtained from the PUSER flagship store. Its main function is to receive RS485 signals from the hub, convert them into JSON format, and then transmit the converted JSON data to the control system using the MQTT protocol.

In terms of actuators, the system is equipped with PTC heaters and semiconductor coolers to adjust the temperature. To optimize the circulation of cold and warm air, the heater is installed in the lower part of the greenhouse, while the cooler is installed in the upper part. In addition, ventilation fans are included to provide effective air circulation. To control the air humidity in the greenhouse, the system is equipped with an ultrasonic humidifier, supplemented by fans to enhance the humidification effect. The fan installed next to the humidifier helps to evenly distribute the misted moisture throughout the greenhouse, ensuring uniform humidity.

Table 1

Hardware Equipment

Equipment	Models	Producers
soil sensor	VMS-3001-TR-*	VEMSEE Flagship Store
air sensor	VMS-3002-WS	VEMSEE Flagship Store
hub	HM-RS485-16-JX	eMybos
gateway	USR-M100	PUSER Flagship Store
heater	DJR	Kunli Electric
cooler	12V Semiconductor Chiller	ZeJie
humidifier	SHILU-12568	ShiLu
fan	15050-17251	SanXie

Greenhouse structure

The greenhouse frame is shown in Figure 1. It is constructed from 3-mm thick acrylic panels, providing good light transmission for plant growth. The greenhouse was designed in a square shape with a length of 800 mm, a width of 600 mm and a height of 700 mm. Ventilation openings with a diameter of 150 mm are provided on both sides to facilitate air circulation. The top of the greenhouse is provided with three square holes 47 mm long to hold the cooler and the bottom is provided with mounting holes 5 mm in diameter for the heater. To further ensure temperature stability, an insulating film was added to the exterior of the greenhouse to improve thermal efficiency and minimize heat loss.

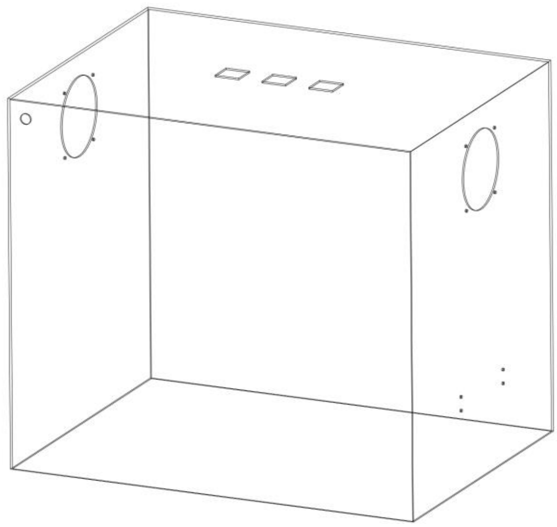

Fig. 1 - Greenhouse frame

System architecture

The overall conceptual diagram of the proposed system is shown in Figure 2. The system architecture consists of three main components: an environmental monitoring system, a control system and a data visualization platform. The primary function of the environmental monitoring system is to collect, transmit and initially process environmental data. The system comprises six RS485 sensor nodes and one edge gateway.

Each sensor is connected to the hub via an RS485 interface and communicates with the edge gateway through a serial port. The edge gateway is responsible for receiving environmental data from the hub performing initial processing and converting the data format. First, it receives sensor data such as temperature and humidity from the hub via a pre-configured interface, encapsulates the data into JSON format, and sends the JSON data to the specified MQTT topic via the MQTT protocol. The system utilizes the ESP8266 Wi-Fi module to connect to the MQTT server and subscribe to the topic to receive the environmental data. The received JSON data is transferred through serial communication to STM32F103ZET6 microcontroller, which is responsible for processing and analysing the received data. It compares the real-time data with the pre-set parameters to determine if the environmental conditions are within the expected range. Based on the comparison results, the control system adjusts the duty cycle of the PWM (pulse width modulation) signal to fine-tune the system's response. By modulating the PWM signal, the switching state of the electromagnetic relay is controlled, which in turn regulates actuators such as fans, heaters, coolers, etc., ensuring real-time monitoring and fine-tuning of environmental parameters.

The data visualization platform adopts MVVM (Model- View - ViewModel) separation framework for the front-end and back-end, which ensures the modularity and efficiency of the system. The back-end is implemented using the Django Channels framework, which is mainly responsible for processing the data received from the edge gateway and facilitating real-time communication with the front-end via WebSocket (*Fuentes et al., 2024*). The front-end is implemented using a JavaScript framework, which receives the data pushed from the back-end via WebSocket and updates the display interface in real time. The data is finally stored in a MySQL database for post-processing and analysis. The whole system is designed to be efficient and reliable, ensuring that users can monitor environmental data in real time and respond in a timely manner.

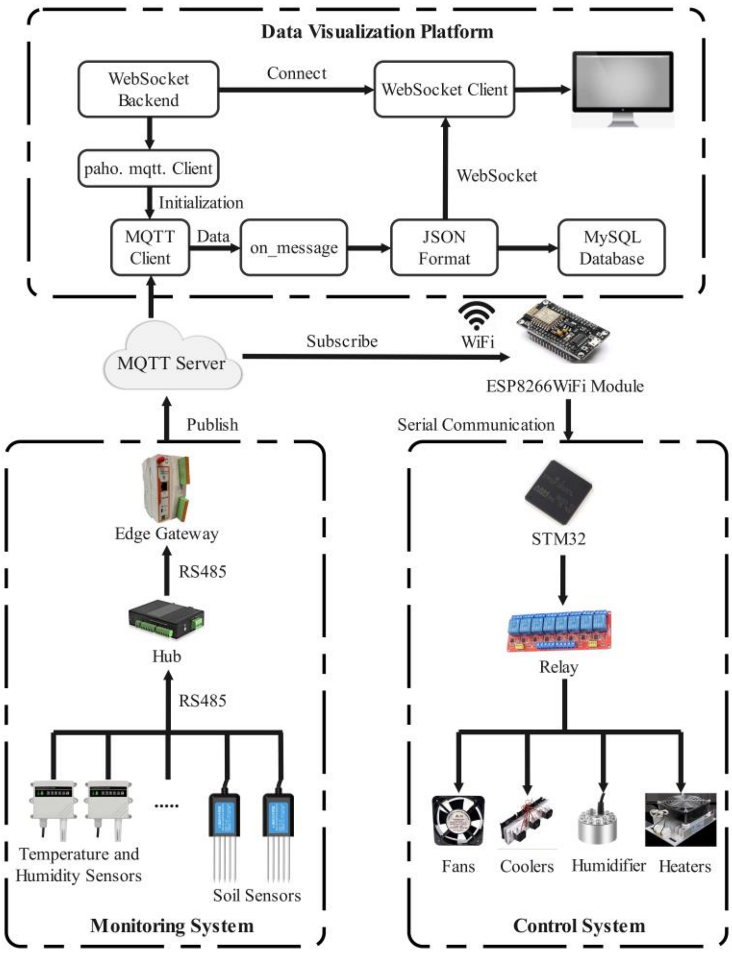

Fig. 2 - System framework

Optimization of fuzzy PID control parameters based on APSO

PSO is a global optimization algorithm that simulates the foraging behaviour of a flock of birds and searches for an optimal solution by updating the positions and velocities of each particle in the population. PSO relies on fixed parameter settings (e.g., inertia weights and learning factors), which are adjusted by the guidance of the individual optimums and global optimums during the search process (*Chen and Chi, 2010*). In a traditional PSO, the formula for updating the velocity and position of each particle is:

$$\mathrm{v}_i(t+1) = w \cdot v_i(t) + c_1 \cdot r_1 \cdot (pdest_i - x_i) + c_2 \cdot r_2 \cdot (gbest - x_i) \tag{1}$$

$$x_i(t+1) = x_i(t) + v_i(t+1) \tag{2}$$

where:

v_i is the velocity of particle i; x_i is the position of particle i; w is the inertia weight, which is used to control the velocity of the particle; c_1, c_2 is the learning factor; r_1, r_2 is a random number in the range of [0,1]; $pdest_i$ is the historical optimal position of particle i; and $gbest$ is the historical optimal position of the whole particle.

However, traditional PSO is prone to fall into local optimal solutions and is sensitive to parameter settings *(Pan et al., 2020*). The APSO algorithm introduces a dynamic adjustment mechanism on this basis, which automatically adjusts the inertia weights, learning factors and other parameters according to the current search stage, making the algorithm more flexible in balancing the global and local searches, improving the search efficiency and robustness of the algorithm, and reducing the probability of falling into a local optimum (*Weng et al., 2024*). In optimizing the parameters of the fuzzy PID controller, APSO can accurately adjust the proportional (*KP*), integral (KI), and differential (KD) coefficients, which makes the controller more adaptable and robust in the face of complex, nonlinear, and time-varying systems (*Liu, 2016*).

First, the position and velocity of the particle swarm are initialized. The initial position of each particle represents a set of PID control parameters. The velocity of the particle determines the step size and direction of its search, and the initial velocity is typically set to a random value. The position and velocity of the particle are respectively:

The position and velocity of the particle are given by:

$$x_i = (KP, KI, KD) \tag{3}$$

$$v_i = (v_{KP}, v_{KI}, v_{KD}) \tag{4}$$

where: i denotes the number of the particle.

APSO primarily enhances the search ability of particle swarms and optimizes the convergence speed by dynamically adjusting inertial weights and learning factors, thereby improving the search efficiency of the global optimal solution and reduces the likelihood of falling into the local optimal solution.

The inertia weight controls the relationship between the particle's current speed and its previous speed, and determines the particle's "inertia". The inertia weight is generally reduced during the iteration process so that particles can conduct extensive searches in the early iterations and then focus their searches in the later iterations to converge to the global optimal solution.

The calculation formula is as follows:

$$W = w_{\max} - \frac{(w_{\max} - w_{\min})}{T_{\max}} T \tag{5}$$

where:

w_{max} is the initial inertia weight; w_{min} - minimum inertia weight; T_{max} - maximum number of iterations;

T - current number of iterations.

The learning factor controls the speed at which particles approach their personal optimal solution and the global optimal solution, determining the dependency of particle search. Usually, the PSO algorithm uses two learning factors: one is the individual learning factor and the other is the group learning factor. The individual learning factor controls how the particle depends on its own historical experience, that is, how the particle adjusts its current speed according to the optimal position it has reached.

The group learning factor controls how the particle depends on the global experience of the group, that is, how the particle adjusts its current speed according to the optimal solution in the group.

The specific adjustment formula is:

$$c_1(t) = c_{1,\max} - \frac{(c_{1,\max} - c_{1,\min})}{T} \cdot t \tag{6}$$

$$c_2(t) = c_{2,\max} - \frac{(c_{2,\max} - c_{2,\min})}{T} \cdot T \tag{7}$$

where:

$c_{1,\ max}$, $c_{2,\ max}$ - maximum value of the learning factor; $c_{1,\ min}$, $c_{2,\ min}$ - minimum value of the learning factor; t -current number of iterations; T - maximum number of iterations.

The standard random number in PSO can lead to search restrictions in the particle update process, increasing the likelihood of falling into local optimal solution, especially when the solution space is complex and the dimension is high. After the introduction of Levy flight, a random term with heavy-tail distribution is usually used to replace the original random numbers r1 and r2, so that the particle position update is no longer determined only by uniform random numbers, but a "heavy-tail jump" mechanism is introduced. The update formula is as follows:

$$\mathrm{v}_i(t+1) = w \cdot v_i(t) + c_1 \cdot L_1 \cdot (pdest_i - x_i) + c_2 \cdot L_2 \cdot (gbest - x_i) \tag{8}$$

where:

L_1 and L_2 are random numbers generated based on Levy distribution, following a heavy-tailed distribution. These random numbers are usually generated through the distribution formula of Levy flight, which is characterized by occasional large jumps to help particles perform global search.

RESULTS

Model identification

A PTC heater was installed at the base of the small-scale greenhouse, complemented by fans mounted symmetrically at the top. Temperature and humidity sensors were positioned at different locations within the greenhouse, and different target temperatures are set to simulate the operational process of the greenhouse and infer its transfer function model. In the closed greenhouse model, the ambient temperature is approximately 25.4°C, and the target temperature is set to 30.0°C. When the ambient temperature has not reached the target value, the heater will continue to operate; if the temperature exceeds the target value, the ventilation fan will be activated to cool the environment. Temperature data is recorded once per second over a period of 750 seconds.

To identify the system model, the recorded sample data was imported into the MATLAB/Simulink environment to determine the system's transfer function. The System Identification Toolbox in MATLAB, employing the nonlinear least squares method, is used for this process. The best fit value is calculated using the following formula: after importing the collected temperature data into MATLAB, the System Identification Toolbox in Simulink applies the least squares method to analyse and identify the system’s transfer function.

The model's best fit R^2 is calculated using the following equation:

$$R^2 = 1 - \frac{\sum(\mathrm{y}-\mathrm{y}_m)^2}{\sum(\mathrm{y}-\bar{\mathrm{y}})^2} \tag{9}$$

where:

R^2 represents the model's best fit, y is the actual recorded temperature data, y_m is the predicted temperature data based on the identified transfer function model, and $\bar{\mathrm{y}}$ is the mean of the actual temperature data.

This equation evaluates the model's accuracy by calculating the ratio between the sum of the squared errors between the predicted values and the actual measurements (numerator) and the total variance of the actual measurements from their mean (denominator). If the R^2 value approaches 100%, it indicates that the identified transfer function model fits the actual data well; conversely, a lower R^2 value suggests a poorer fit. As shown in Figure 3, the output temperature of the greenhouse system and the fitted curve are presented.

The resulting fitted curve is as follows:

$$G(s) = \frac{4.87}{151s+1}e^{-30s} \tag{10}$$

the fit of the curve is: 94.54%

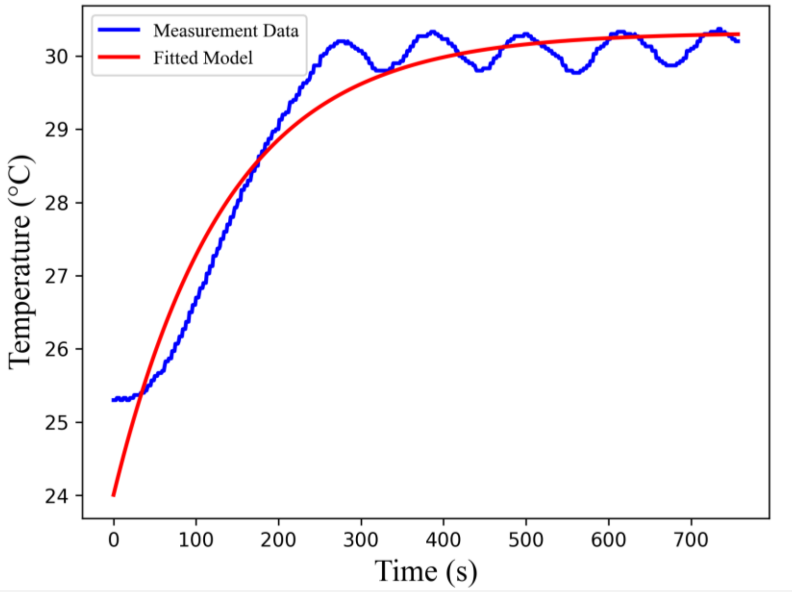

Fig. 3 - Real-time temperature parameters and fitted curves

Fuzzy control strategy and rules

In accordance with the principles of the fuzzy PID control algorithm, the inputs to the fuzzy PID controller are the error and the rate of *E* and the rate of error *Ec*. These inputs are crucial for the controller to assess the system's deviation from the desired setpoint. The outputs of the fuzzy PID controller correspond to the adjustments of the proportional, integral, and derivative gains, represented as ΔKP, ΔKI, and ΔKD. As shown in Table 2, the fuzzy domains for E, Ec, KP, KI, KD are [-6, 6], [-6, 6], [-3, 3], [-0.3, 0.3], and [-0.3, 0.3], respectively. The fuzzy subsets are PB, PM, PS, ZO, NS, NM, and NB. The membership functions for the inputs E and Ec are shown in Figures 4 (a) and (b), while the membership functions for the outputs ΔKP, ΔKI, and ΔKD are depicted in Figure 4(c), (d), and (e), respectively.

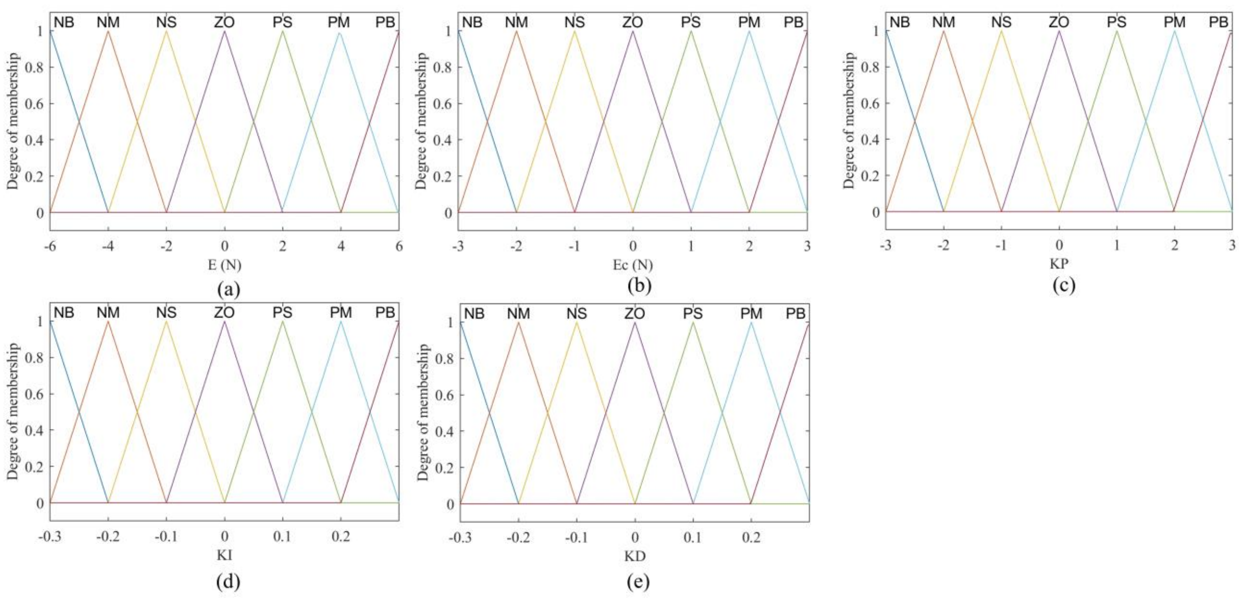

Fig. 4 - Domain and membership function of (a) E, (b) Ec, (c) △KP、(d) △KI and(e) △KD

Table 2

Fuzzy quantization parameters for input and output quantities

Variable	E	Ec	KP	KI	KD
Fuzzy discourse domain	[−6,6]	[−6,6]	[-3,3]	[-0.3,0.3]	[-0.3,0.3]
Fuzzy subset	PB, PM, PS, ZO, NS, NM, NB				
Membership function	Trimf				

The fuzzy rule base is composed of several "if-then" rules, where each rule is designed for specific input conditions and corresponding outputs. The input variables—*E* and *Ec*—are fuzzified into different linguistic variables, while the output variables represent adjustments to the PID controller parameters. Based on different combinations of error *E* and error rate *Ec*, 49 strategies and rules have been developed for adjusting *ΔKP*, *ΔKI*, and *ΔKD* in the fuzzy PID control system, as shown in Table 3. The input-output characteristic surfaces are presented in Figure 5 (a), (b), and (c).

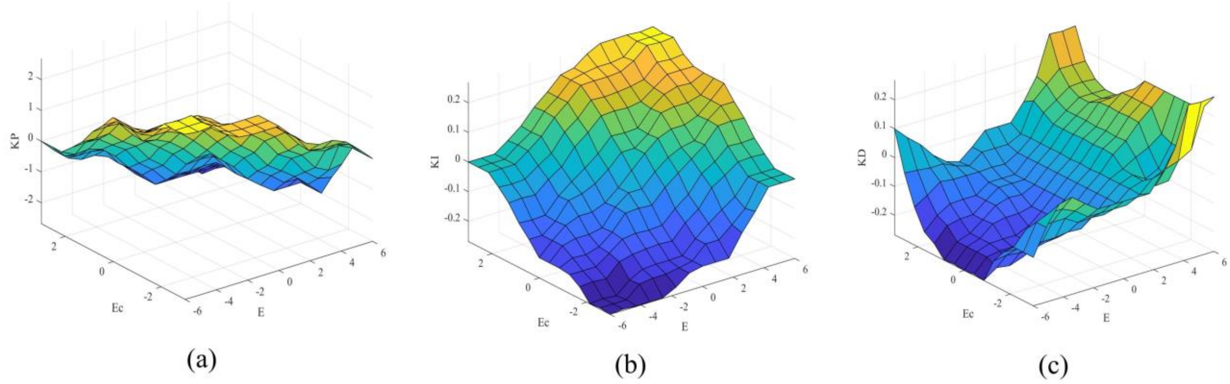

Fig. 5 - Input and output characteristic surfaces of (a) △KP, (b) △KI, (c) △KD

Table 3

Fuzzy control rules

E	*Ec*						
	NB	**NM**	**NS**	**ZO**	**PS**	**PM**	**PB**
NB	PB, NB, NS	PB, NB, NS	PM, NM, NB	PM, NM, NB	PS, NS, NB	ZO, ZO, NM	ZO, ZO, PS
NM	PB, NB, NS	PB, NB, NS	PM, NM, NB	PS, NS, NM	PS, NS, NM	ZO, ZO, NS	NS, ZO, ZO
NS	PM, NB, ZO	PM, NM, NS	PM, NS, NM	PS, NS, NM	ZO, ZO, NS	NS, PS, NS	NS, PS, NS
ZO	PM, NM, ZO	PM, NM, NS	PS, NS, NS	ZO, ZO, NS	NS, PS, NS	NM, PM, NS	NM, PM, ZO
PS	PS, NM, ZO	PS, NS, ZO	ZO, ZO, ZO	NS, PS, ZO	NS, PS, ZO	NM, PM, ZO	NM, PB, ZO
PM	PS, ZO, PB	ZO, ZO, NS	NS, PS, PS	NM, PS, PS	NM, PM, PS	NM, PB, PS	NB, PB, PB
PB	ZO, ZO, PB	ZO, ZO, PM	NM, PS, PM	NM, PM, PM	NM, PM, PS	NB, PB, PS	NB, PB, PB

Simulation and experimental results

The structure of the APSO fuzzy PID controller is shown in Figure 6. The APSO algorithm is executed to optimize the three parameters of the fuzzy PID controller, and the resulting optimization curve is presented in Figure 8 (a) - (e).

The optimization process illustrates the trend of each parameter across multiple iterations. As the number of iterations increases, the parameters gradually stabilize, indicating that the APSO algorithm effectively adjusts the particle swarm's search strategy and quickly finds the optimal control parameters. The fitness variation curve is shown in Figure 8 (f). From the curve, it can be observed that the APSO algorithm performs a global search in the initial stage, identifies a better solution within a short time, and then gradually converges to the optimal solution.

During the system simulation, the initial temperature of the greenhouse was set to 30°C, and the simulation time was set to 750 seconds. The performance of APSO fuzzy PID control, fuzzy PID control, and traditional PID control were compared. As shown in Figure 7, during the dynamic response phase, the APSO-optimized fuzzy PID control method significantly reduces the oscillation amplitude and frequency compared to the PID and fuzzy PID methods. This effectively improves the dynamic characteristics of the system and ensures that the response curve meets the control requirements.

By analysing the fluctuation curves of the simulation experiments using a MATLAB oscilloscope, the time domain performance metrics can be derived and the results are shown in Table 4. Compared to fuzzy PID and PID, APSO fuzzy PID reduces overshoot by 22.8% and 72.1%, respectively; the adjustment time is reduced by 9% and 20%, respectively; and the system's stability is significantly improved. By observing the oscilloscope waveform, it is evident that the optimized controller can quickly identify and effectively suppress the influence of disturbances, allowing the system output to return to a stable state in a short time. This demonstrates that the fuzzy PID controller optimized by APSO has strong anti-disturbance capability, enabling the system to maintain high control accuracy and robustness under interference.

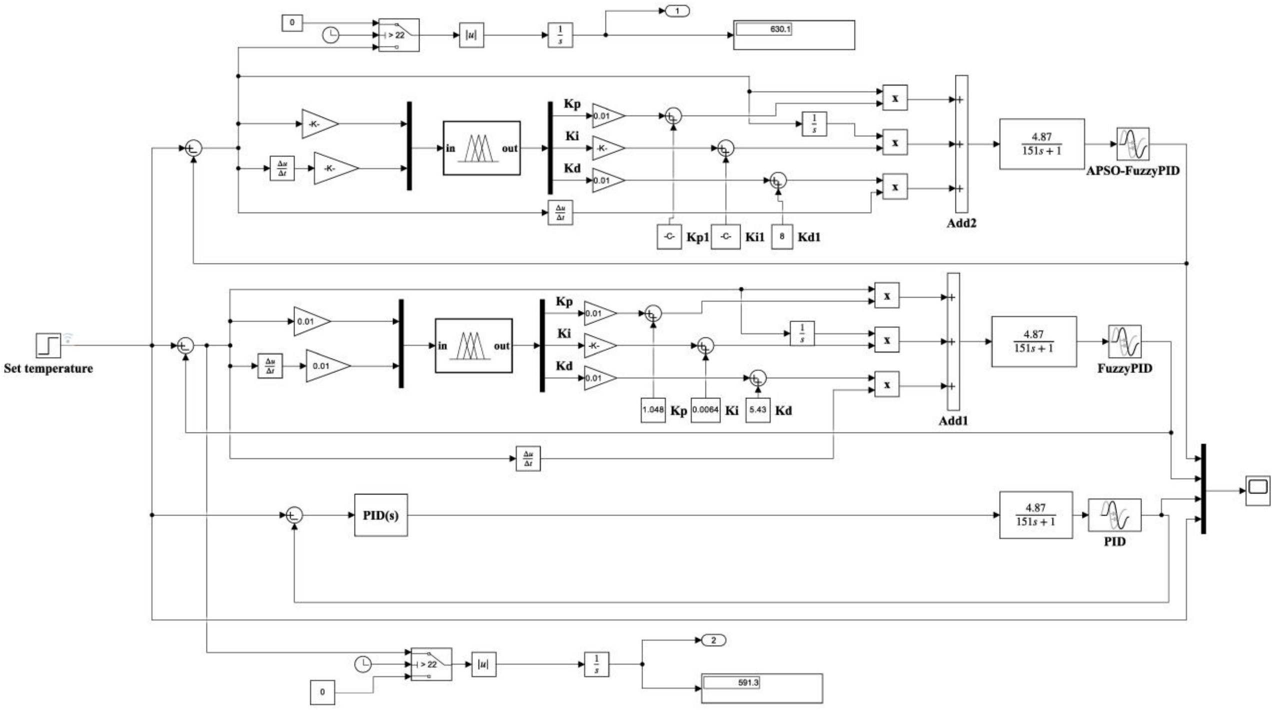

Fig. 6 - System controller

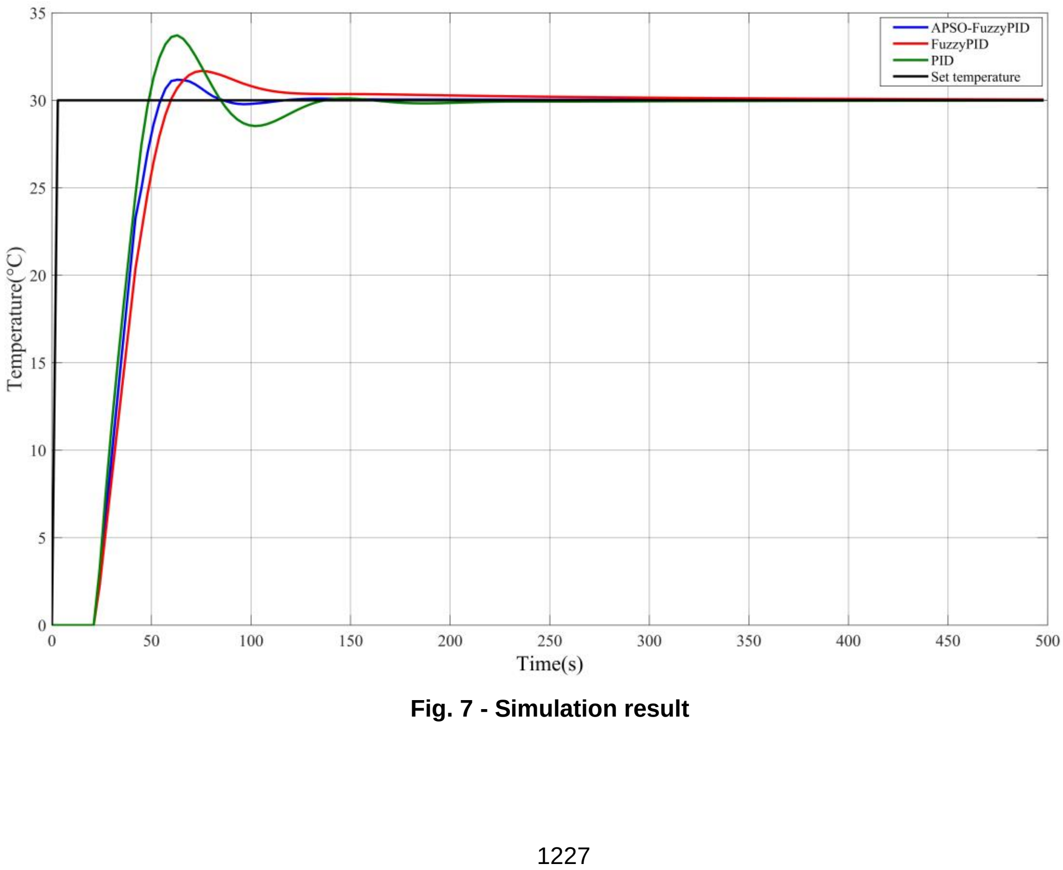

Fig. 7 - Simulation result

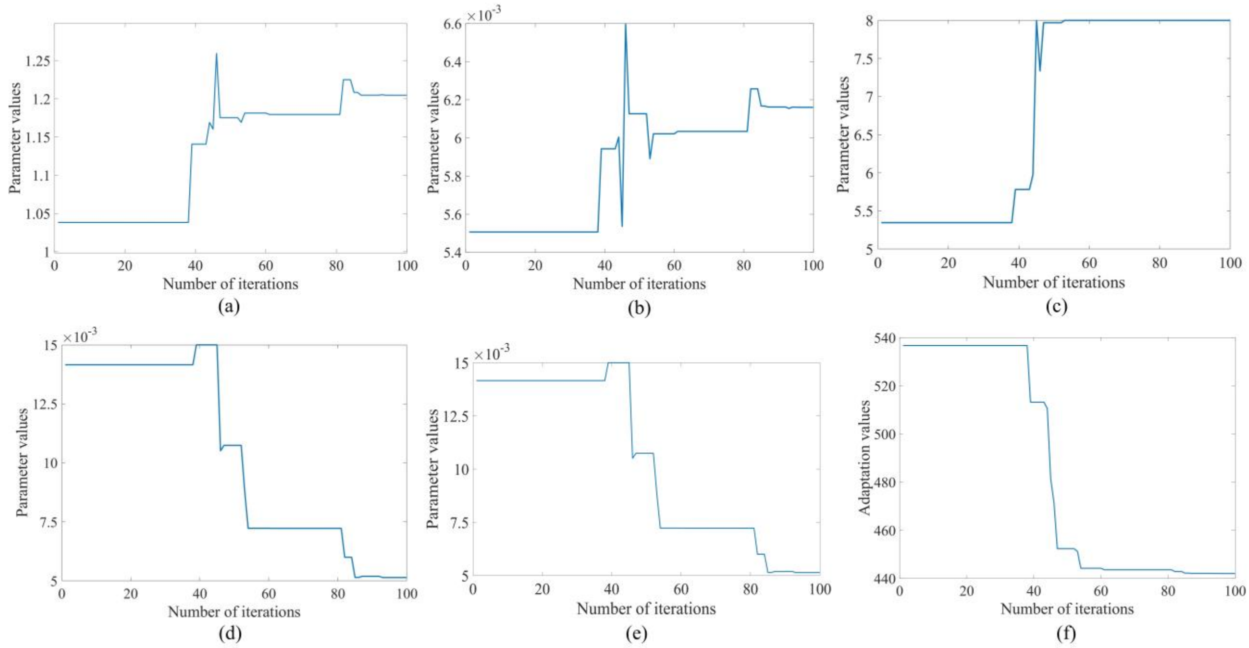

Fig. 8 - (f) Adaptation changes curves; parameter optimization results (a): KP, (b): KI, (c): KD, (d): Ke, (e): Kec.

Table 4

Analysis of simulation results

Performances	Methodologies		
	APSO Fuzzy PID	Fuzzy PID	PID
Rising time t_r/s	23.8	27.7	20.6
Overshoot σ/%	3.65%	4.73%	13.07%
Adjustment time t_s/s	110.1	121	137.5

The structural layout of the greenhouse is depicted in Figure 9. Three air temperature and humidity sensors were placed around the greenhouse to monitor the overall temperature, while a soil parameter sensor was embedded in the soil to monitor soil conditions. Two fans were symmetrically installed to facilitate air circulation, and the heater and cooler were installed in the upper and lower parts of the greenhouse, respectively, to control the temperature.

Fig. 9 - Greenhouse structure

In this experiment, the effectiveness of the greenhouse control system was tested at set temperatures of 24°C, 28°C, and 30°C, as shown in Figure 10 (a), (b), and (c). Throughout the experiment, the internal temperature of the greenhouse was continuously adjusted and monitored in real time using a precise environmental control system. The results showed that the temperature control system in the greenhouse responded quickly and remained near the set point, with fluctuations within 0.3°C. This demonstrates the system's strong temperature regulation capability, effectively maintaining the required temperature range and ensuring the stability of the greenhouse environment. In terms of humidity control, the greenhouse humidity was regulated using direct control methods, as ambient humidity decreases slowly. The experimental results are shown in Figure 10 (d).

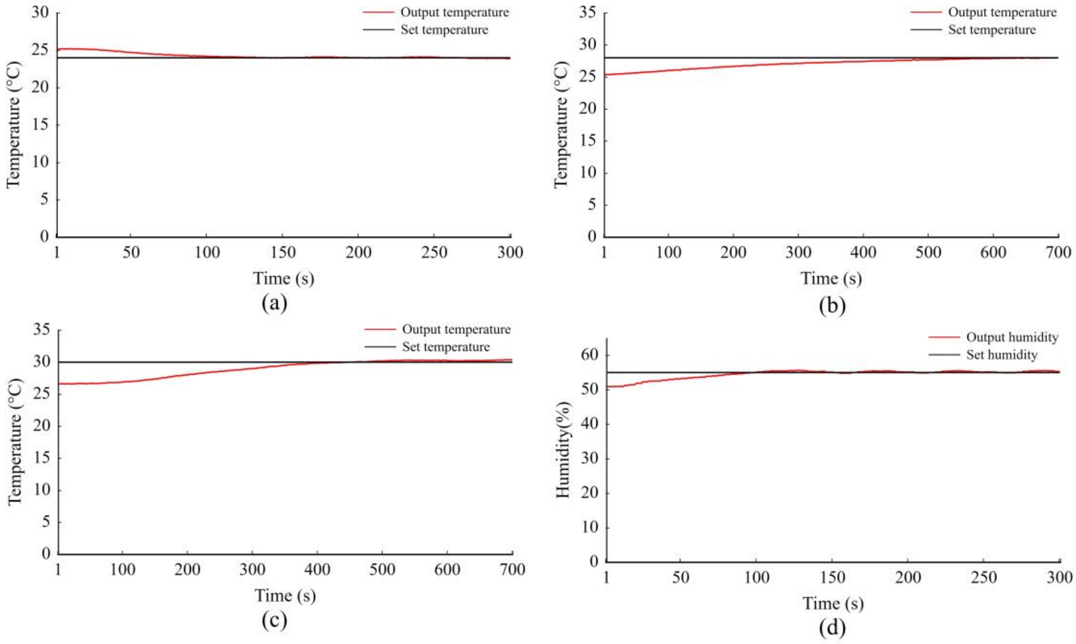

Fig. 10 - Temperature control curves at (a) 24°C, (b) 28°C, (c) 30°C, (d) 55% Humidity

The performance tests of the system at outside temperatures of 22°C and 17°C are shown in Figure 11 (a) and (b), respectively. The test results revealed that as the ambient temperature decreased, the system's response time extended accordingly; however, this did not affect the overall control effectiveness. To evaluate the system's performance under varying humidity conditions, tests were conducted at greenhouse humidity levels of 30%, 40%, 50%, and 60%, with the results displayed in Figure 11 (c), (d), (e), and (f). The results showed that the different humidity levels had almost no effect on the system's responsiveness or its stabilizing effect.

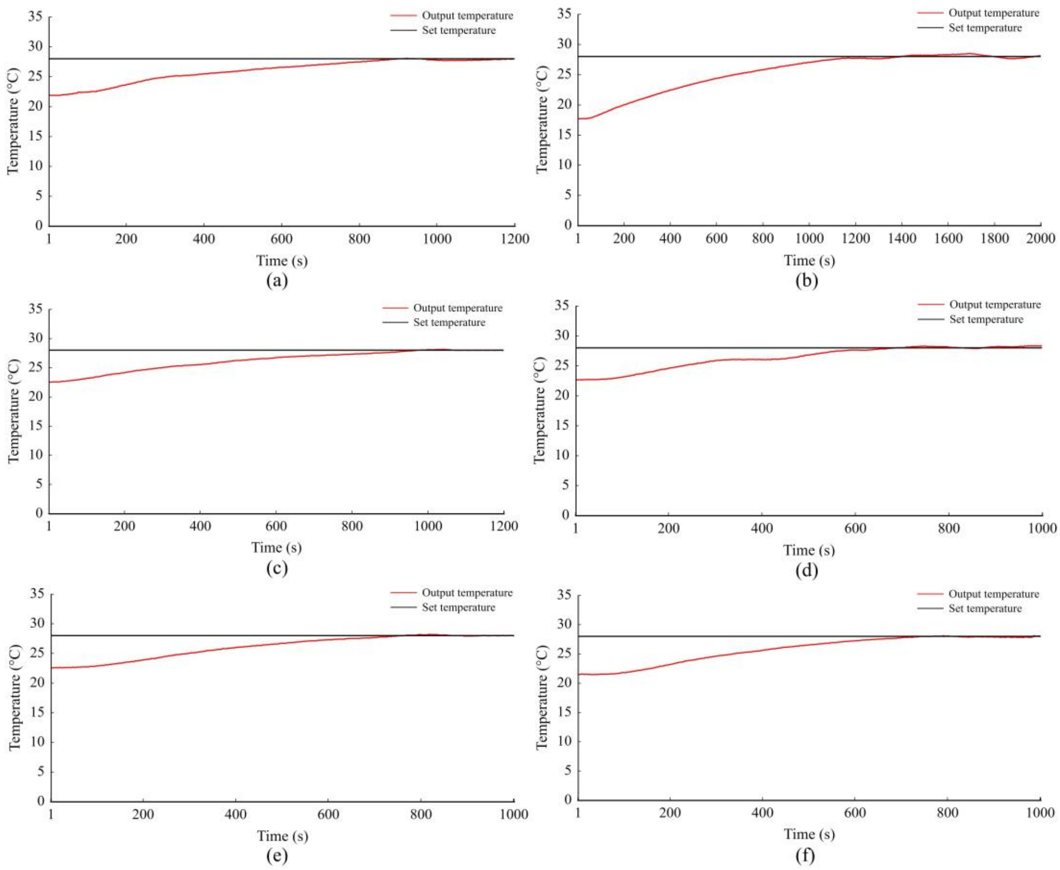

Fig. 11- Control effect at different ambient temperatures: (a) 22°C, (b) 17°C; control effect at different humidity: (c) 30%, (d) 40%, (e) 50%, (f) 60%

The configured data visualization platform, shown in Figure 12, clearly displays various environmental parameters within the greenhouse, including temperature, humidity, soil salinity, and pH. The platform is also equipped with an anomaly alert function, which automatically triggers an alarm when any environmental parameter exceeds the preset safety range, prompting the user to take timely action. Figure 13 shows the developed MySQL database, which allows different data to be stored for later analysis and processing.

Fig. 12 - Data presentation platform

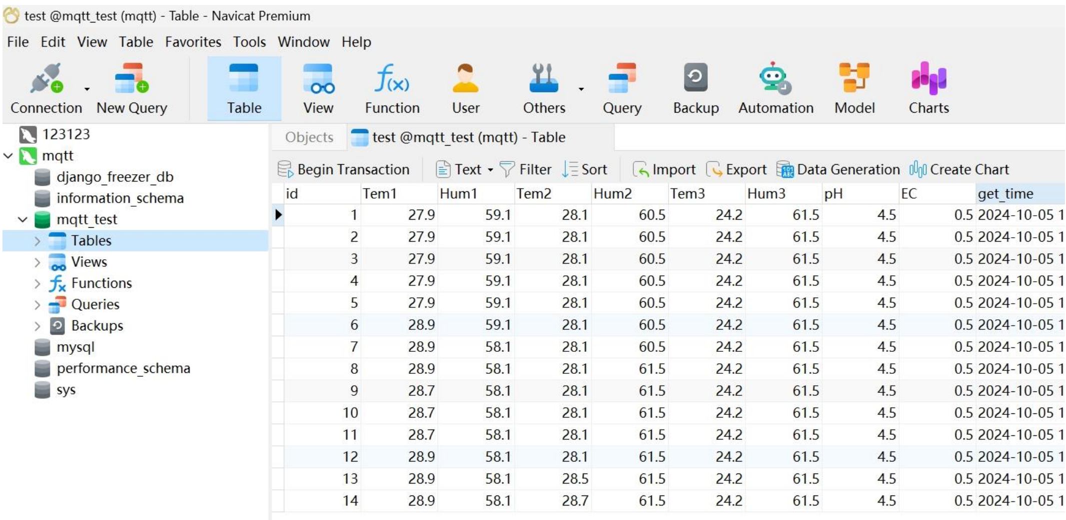

id	Tem1	Hum1	Tem2	Hum2	Tem3	Hum3	pH	EC	get_time
1	27.9	59.1	28.1	60.5	24.2	61.5	4.5	0.5	2024-10-05 1
2	27.9	59.1	28.1	60.5	24.2	61.5	4.5	0.5	2024-10-05 1
3	27.9	59.1	28.1	60.5	24.2	61.5	4.5	0.5	2024-10-05 1
4	27.9	59.1	28.1	60.5	24.2	61.5	4.5	0.5	2024-10-05 1
5	27.9	59.1	28.1	60.5	24.2	61.5	4.5	0.5	2024-10-05 1
6	28.9	59.1	28.1	60.5	24.2	61.5	4.5	0.5	2024-10-05 1
7	28.9	58.1	28.1	60.5	24.2	61.5	4.5	0.5	2024-10-05 1
8	28.9	58.1	28.1	61.5	24.2	61.5	4.5	0.5	2024-10-05 1
9	28.7	58.1	28.1	61.5	24.2	61.5	4.5	0.5	2024-10-05 1
10	28.7	58.1	28.1	61.5	24.2	61.5	4.5	0.5	2024-10-05 1
11	28.7	58.1	28.1	61.5	24.2	61.5	4.5	0.5	2024-10-05 1
12	28.9	58.1	28.1	61.5	24.2	61.5	4.5	0.5	2024-10-05 1
13	28.9	58.1	28.5	61.5	24.2	61.5	4.5	0.5	2024-10-05 1
14	28.9	58.1	28.7	61.5	24.2	61.5	4.5	0.5	2024-10-05 1

Fig. 13 - MySQL database

CONCLUSIONS

This study focused on the design and implementation of a greenhouse environmental control system, with an in-depth investigation of a fuzzy control-based temperature regulation strategy and the integration of an intelligent display platform for environmental monitoring. Through experimental validation, the greenhouse environment achieved stable and precise control under different temperature settings, confirming the effectiveness of the fuzzy control method in managing complex nonlinear systems. In addition, the constructed big data display platform successfully collected and visualized greenhouse parameters such as temperature and humidity in real time, providing managers with intuitive and detailed environmental information. Moreover, the platform included an anomaly alert feature that could promptly identify and notify users of potential environmental risks, thereby enhancing the safety and automation of greenhouse management.

Future work will focus on optimizing the control algorithms for broader deployment, integrating more diverse environmental sensors, and enhancing the robustness of the platform under varying network conditions. This study not only validated the efficacy of fuzzy control in greenhouse environmental management but also demonstrated the broad application potential of intelligent display platforms in agricultural management.

The system ensures the stability of the crop growth environment while simplifying management processes and reducing the need for manual intervention, providing strong support for the intelligent and precise development of modern agriculture.

ACKNOWLEDGEMENT

This work was supported by the National Natural Science Foundation of China (32372438, 31772068, 31872909, 32111530291, 32281240407), Funding Project for the Central Government to Guide the Development of Local Science and Technology (YDZX2022163), Technological Innovation Guidance Project of Department of Science & Technology of Gansu Province (22CX8NA023). The authors also extended their appreciation to the Researchers Supporting Project number (RSPD2025R944), King Saud University, Riyadh, Saudi Arabia, for funding this work.

REFERENCES

[1] Akaev A. (2022). Phenomenological models of the global demographic dynamics and their usage for forecasting in 21st century. *Applied Mathematics*, 13(7), 612-49. https://doi.org/10.4236/am.2022.137039

[2] Atia D. M., El-madany H. T. (2017). Analysis and design of greenhouse temperature control using adaptive neuro-fuzzy inference system. *Journal of Electrical Systems and Information Technology*, 4(1), 34-48. https://doi.org/10.1016/j.jesit.2016.10.014

[3] Chen T. Y., Chi T. M. (2010). On the improvements of the particle swarm optimization algorithm. *Advances in Engineering Software*, 41(2), 229-39. https://doi.org/10.1016/j.advengsoft.2009.08.003

[4] Cheng Y. (2020). Research on intelligent control of an agricultural greenhouse based on fuzzy PID control. *Journal of Environmental Engineering and Science*, 15(3), 113-18. https://doi.org/10.1680/jenes.19.00054

[5] Chin J., Callaghan V., Allouch S. B. (2019). The Internet-of-Things: Reflections on the past, present and future from a user-centered and smart environment perspective. *Journal of Ambient Intelligence and Smart Environments*, 11(1), 45-69. https://doi.org/10.3233/AIS-180506

[6] Fadhel M. A., Duhaim A. M., Albahri A., Al-Qaysi Z., Aktham M., Chyad M., Abd-Alaziz W., Albahri O., Alamoodi A., & Alzubaidi L. (2024). Navigating the metaverse: unraveling the impact of artificial intelligence—a comprehensive review and gap analysis. *Artificial Intelligence Review*, 57(10), 264. https://doi.org/10.1007/s10462-024-10881-5

[7] Fuentes J. M., Silva M., Muñoz C., Reyes H., Bustamante-Encina R., & Gatica G. (2024). Georeferenced environmental platform for kindergarten monitoring based on internet of things and websockets. *Procedia Computer Science*, 231, 629-35. https://doi.org/10.1016/j.procs.2023.12.172

[8] Gatkal N. R., Nalawade S. M., Sahni R. K., Bhanage G. B., Walunj A. A., Kadam P. B., & Ali M. (2024). Review of IoT and electronics enabled smart agriculture. *International Journal of Agricultural and Biological Engineering*, 17(5), 1-14. https://doi.org/10.25165/j.ijabe.20241705.8496

[9] Goli I., Kriaučiūnienė Z., Zhang R., Bijani M., Kabir Koohi P., Rostamkalaei S. A., Lopez-Carr D., & Azadi H. (2024). Contributions of climate smart agriculture toward climate change adaptation and food security: The case of mazandaran province, Iran. *Trends in Food Science & Technology*, 104653. /https://doi.org/10.1016/j.tifs.2024.104653

[10] Hemathilake D., Gunathilake D. (2022). Agricultural productivity and food supply to meet increased demands. *Future Foods*, 539-53. https://doi.org/10.1016/B978-0-323-91001-9.00016-5

[11] Katzin D., Van Henten E. J., Van Mourik S. (2022). Process-based greenhouse climate models: Genealogy, current status, and future directions. *Agricultural Systems*, 198, 103388. https://doi.org/10.1016/j.agsy.2022.103388

[12] Khondoker M., Mandal S., Gurav R., & Hwang S. (2023). Freshwater shortage, salinity increase, and global food production: A need for sustainable irrigation water desalination—A scoping review. *Earth*, 4(2), 223-40. https://doi.org/10.3390/earth4020012

[13] Kumar L., Chhogyel N., Gopalakrishnan T., Hasan M. K., Jayasinghe S. L., Kariyawasam C. S., Kogo B. K., & Ratnayake S. (2022). Climate change and future of agri-food production. *Future Foods*, 2022, 49-79. https://doi.org/10.1016/B978-0-323-91001-9.00009-8

[14] Lee S. Y., Lee I. B., Yeo U. H., Kim R. W., & Kim J. G. (2019). Optimal sensor placement for monitoring and controlling greenhouse internal environments. *Biosystems Engineering*, 188, 190-206. https://doi.org/10.1016/j.biosystemseng.2019.10.005

[15] Márquez-Vera M. A., Ramos-Fernández J. C., Cerecero-Natale L. F., Lafont F., Balmat J.-F., & Esparza-Villanueva J. I. (2016). Temperature control in a MISO greenhouse by inverting its fuzzy model. *Computers and electronics in Agriculture*, 124, 168-74. https://doi.org/10.1016/j.compag.2016.04.005

[16] Mohamed T. M. K., Gao J., Tunio M. (2022). Development and experiment of the intelligent control system for rhizosphere temperature of aeroponic lettuce via the Internet of Things. *International Journal of Agricultural and Biological Engineering*, 15(3), 225-33. https://doi.org/10.25165/j.ijabe.20221503.6530

[17] Omasa K., Ono E., Ishigami Y., Shimizu Y., & Araki Y. (2022). Plant functional remote sensing and smart farming applications. *International journal of agricultural and biological engineering*, 15(4), 1-6. https://dx.doi.org/10.25165/j.ijabe.20221504.7375

[18] Pan Y., Chen J., Yuan Z. (2020). Research on intelligent ship path planning optimization based on chaos particle swarm optimization. *International Core Journal of Engineering*, 6, 407-16. https://doi.org/10.6919/ICJE.202012_6(12).0057

[19] Schoder D. (2018). Introduction to the internet of things. Internet of Things A to Z: Technologies and Applications. *Wiley*.

[20] Thomopoulos V., Tolis F., Blounas T.-F., Tsipianitis D., & Kavga A. (2024). Application of fuzzy logic and IoT in a small-scale smart greenhouse system. *Smart Agricultural Technology*, 8, 100446. https://doi.org/10.1016/j.atech.2024.100446

[21] van Dijk M., Morley T., Rau M. L., & Saghai Y. (2021). Systematic review and meta-analysis of global food security projections to 2050. *Research Square*. https://doi.org/10.21203/rs.3.rs-530565/v1

[22] Wang L., Zhang H. (2018). An adaptive fuzzy hierarchical control for maintaining solar greenhouse temperature. *Computers and electronics in agriculture*, 155, 251-56. https://doi.org/10.1016/j.compag.2018.10.023

[23] Weng H., Zhu W., Wu J. (2024). Multi mode coordinated control algorithm for DC near-field photovoltaic based on adaptive mutation particle swarm optimization. *Ain Shams Engineering Journal*. 103168. https://doi.org/10.1016/j.asej.2024.103168

[24] Zhang Z., Jiang Y., Zhang S., Geng S., Wang H., & Sang G. (2014). An adaptive particle swarm optimization algorithm for reservoir operation optimization. *Applied Soft Computing*, 18, 167-77. https://doi.org/10.1016/j.asoc.2014.01.034

[25] Zheng W., Meng F., Liu N., & Huang S. (2023). A game model for analyzing wireless sensor networks of 5G environment based on adaptive equilibrium optimizer algorithm. *Sensors*, 23(19), 8055. https://doi.org/10.3390/s23198055

[26] Zhou D., Meinke H., Wilson M., Marcelis L. F. M., & Heuvelink E. (2021). Towards delivering on the sustainable development goals in greenhouse production systems. *Resources, Conservation and Recycling*, 169, 105379. https://doi.org/10.1016/j.resconrec.2020.105379